

Element Status in Rats at Intramuscular Injection of Iron Nanoparticles

Elena Anatolyevna Sizova¹, Elena Vladimirovna Yausheva²,
Sergey Alexandrovich Miroshnikov, Svyatoslav Valerievich Lebedev and
Galimzhan Kalihanovich Duskaev³

Orenburg State University, Russia, 460018, Orenburg, 13 Pobedy Pr. and All-Russian Research Institute of Beef Cattle Breeding, Russia, 460000, Orenburg, 29, 9 Yanvarya St.

²All-Russian Research Institute of Beef Cattle Breeding, Russia, 460000, Orenburg, 29, 9 Yanvarya St. Orenburg State University, Russia, 460018, Orenburg, 13 Pobedy Pr.

³All-Russian Research Institute of Beef Cattle Breeding, Russia, 460000, Orenburg, 29, 9 Yanvarya St.

doi: <http://dx.doi.org/10.13005/bbra/2182>

(Received: 10 June 2015; accepted: 26 August 2015)

The common practice of using iron nanoparticles in human and veterinary medicine as well as their potential use microelement-based medicines determine the need for studying the impact that nanoparticles have on the exchange of chemical elements in the body. The study involved a Wistar rats model using iron nanoparticles (nanoFe) obtained through high-temperature condensation ($d = 80 \pm 5$ nm). The study on genetically engineered luminescent strain *E. coli* K12 TG1 had a pre-installed non-toxic concentration of nanoFe. Atomic emission and mass spectrometry showed the presence of 25 chemical elements in the animals' liver after seven nanoFe intramuscular injections had been given to them. The experiment revealed no disturbance in the liver microstructure. However, an investigation into the dynamics of transaminases (alanine transaminase (ALT), aspartate transaminase (AST)) revealed an increase in their activity. On Day 1 of the experiment the LDH activity went 116.3% up ($p < 0.001$) to go down gradually within 21 days. Intramuscular nanoFe injections came along with certain alteration in the exchange of chemical elements. A single dose of iron nanoparticles caused, in the first seven days, depletion of the liver and its saturation with toxic elements. On the first day after the first injection this was manifested through an increase in the concentration of Pb by 20.0% ($p < 0.05$), Sn by 33.3% ($p < 0.05$), Sr by 66.67% ($p < 0.01$). The most significant adaptive changes in the toxic elements exchange of were observed for Al and Sr. The iron content in the liver decreased on Day 7 after the first injection by 19.35% ($p < 0.05$), Day 2 by 28.9% ($p < 0.05$), Day 3 by 7.01%, Day 7 by 16.79% ($p < 0.05$) compared to the controls. The pool of the macronutrients Ca, K, Mg, Na, P (the sum of the substance amount, mole) was found to vary through the experiment by 4.1–10.4%. Reduction of calcium concentration one day following the first injection (in comparison to the controls) was 6.81%; on Day 7 after the second injection – by 18.58% ($p < 0.05$); after the third and the seventh injections – by 6.1% and 12.4% ($p < 0.01$), respectively. Various studies suggest that there is a need for additional correction of the elemental composition in diets against iron nanoparticles injections.

Keywords: Element Status, Iron Nanoparticles, Rats

The latest years have seen an increase in the research projects pointing at the need for using

iron-containing nanomaterials in Biology and Medicine¹, including magnetic particle visualization^{2,3} in magnetic resonance imaging^{4,5}; in treating cancer^{6,7,8}; in manufacturing biocompatible materials⁹; delivering medicine¹⁰. Iron nanoparticles are viewed as a good alternative to

* To whom all correspondence should be addressed.
Tel: +7-912-344-99-07;
E-mail: Sizova.L78@yandex.ru

the currently available preparations based on this microelement¹¹, etc. Even though iron nanoparticles and its compounds are practically used more and more often there is still no proper understanding of the subcellular impact that these structures have. There facts reporting certain side effect of nanoparticles, which are manifested as disturbed immunity^{12, 13}. Iron and its compounds injections, local or systemic, trigger the development of oxidative stress, which leads to an acute inflammation response¹⁴ and are accompanied with toxicosis in animals¹⁵.

These facts imply comprehensive study of the biological effects caused by the agents based on such nanoparticles. This appears especially urgent in view of the fact that the nanoparticles are promising as commercial microelement agents and possess a number of advantages if matched against mineral salts and organic forms. Selenium nanoparticles, in particular, are less toxic and more effective if compared to selenite and other preparations¹⁶⁻¹⁹.

This explains the interest taken in the impact that iron-containing nanoparticles introduced into the body have on the exchange of other chemical elements. The purpose of this present study is to investigate the effect of iron nanoparticles on microelement exchange in rats.

MATERIALS AND METHODS

Obtaining and notification of iron nanoparticles

Iron nanoparticles (nanoFe) were obtained through high-temperature condensation on a Migen-3 machine²⁰. The nanoparticles were spherical in shape, sized 80 ± 5 nm, Z-potential – 15 ± 0.2 mV. The material notification of the preparations included scanning and transmission electron microscopy using the machines like JSM 7401F, JEM-2000FX (JEOL, Japan); X-ray phase analysis on the diffractometer DRON-7.

The AFM investigation was done on the microscope SMM-2000 (JSC PROTON-MIET, Russia). Through the scanning there were used the cantilevers MSCT-AUNM (Park Scientific Instruments, $\text{N}\text{Ø}\text{Å}$) with a beam stiffness of 0.01 N/m and a needle curvature radius of 15-20 nm. The quantitative morphometric analysis of the obtained images was performed with the actual software for the microscope.

All the experiments were done in triplicate and processed by variation statistics using the software package Statistika V10 RUS). The biological activity and the nanoFe toxicity thresholds were detected through bioluminescence inhibition method. NanoFe samples were prepared at a concentration of 4 mole/l on physiological solution and were ultrasound-treated for 30 minutes (ultrasonic disperser UZDN-2T, (Russia) atf-35 kHz, N 300 W, and A-10 ia). To evaluate the effect of various nanoFe dosages, the resulting suspensions were used to prepare ten serial double dilutions. The genetically engineered luminescent strain *E. coli* K12 TG1 was used; this strain was engineered to constitutively express the luxCDABE genes of the natural marine microorganism *Photobacterium leiognathi* 54D10 and was produced by Immunotech (Moscow, Russia). In prior studies, the strain *E. coli* K12 TG1 was restored by the addition of chilled distilled water. The suspension of bacteria was maintained at $+2-4^{\circ}\text{C}$ for 30 min, after which the temperature of the bacterial suspension was brought to $15-25^{\circ}\text{C}$.

The inhibition of bacterial luminescence was tested by placing the cells in 96-well plates containing the test substance and the suspension of luminescent bacteria in a 1:1 ratio. Subsequently, the tray was placed in the measuring unit of an Infinite PROF200 microplate analyzer (TECAN, Austria), which dynamically registered the luminescence intensity for 180 min at intervals of 5 min.

The effects of the nanomaterials on the intensity of bacterial bioluminescence (I) were evaluated using the formula:

$$I = \frac{I_{k_{0min}} \times I_{o_{nmin}}}{I_{k_{nmin}} \times I_{o_{0min}}}$$

where I_k and I_o are the illumination intensities of the control and experimental samples, respectively, from the 0-th and n -th minutes of measurement. Three threshold levels of toxicity are taken into account:

1. less than 20 – sample is “non-toxic” (luminescence quenching $\leq 20\%$);
2. from 20 to 50 – sample is relatively toxic (luminescence quenching 50%);
3. equal to or greater than 50 – sample toxic (luminescence quenching $\geq 50\%$).

In vivo methods

The research *in vivo* was conducted on male Wistar rats, 150-180 g. The animals were divided into two groups (pair-analogue method used) (n=50). The animals were kept on natural and well-balanced diets typical of rodents. The animals once a week were injected with iron nanoparticle in femoral group of muscles in dosage of 2.0 mg/kg of weight (for 7 weeks, with a total of 7 injections). The control group animals were injected with sterile physiological solution (200 mcl/head). The injection sites were chosen at distances, and in view of the muscle regeneration terms and respective recommendations²¹; repeated injection in the same area was given no earlier than 3 weeks after. The experimental research on animals was done following the instructions set by the respective Russian Regulations (1987) and The Guide for the Care and Use of Laboratory Animals (National Academy Press Washington), D.C., 1996).

The nanoFe injection was prepared through mixing nanoparticles with physiological solution (200 mcl) after which the preparation was sterilized with UV to be further treated with ultrasound for 30 minutes (ultrasonicdispenser UZDN-2T, (Russia) atf-35 kHz, N 300 W, andA-10 ia). The animal biosubstrates were taken at slaughter, which was performed (n=3) by decapitation under Nembutal narcosis 1 and 7 days after each injection.

The element composition of the biosubstrates was studied with atomic emission and mass spectroscopy at the experimental laboratory of the Center for Biotoc Medicine, Moscow, Russia (Registration Certificate of ISO 9001: 2000, Number 4017 – 5.04.06). The biosubstrate ashing was performed with the microwave decomposition system MD-2000 (USA). The element content was determined with the mass-spectrometer Elan 9000 and the atomic emission spectrometer Optima 2000 V (PerkinElmer, USA).

For light microscopy pieces of liver were fixed in a 10 % formalin solution. The paraffin sections (5-6 mcm) were stained with Meyer's hematoxyline-eosin. Iron was detected in the studied organ through Pearls reaction²².

The analysis was done using semi-automatic biochemical analyzer Stat fax 1904 Plus (manufacturer – Awareness Technology Inc, USA)

and commercial kits by Randox (USA).

RESULTS

In vitro study results

The results obtained allowed describing the dynamics of bacterial bioluminescence inhibition through time, as well as demonstrating the link between the registered effects and different concentrations of nanoFe.

NanoFe preparation in a dosage of 0.5 mole/l (28 g/l) resulted in 50 % bacteria luminescence quenching 60 minutes after the contact, if compared with the controls, with complete suppression of bioluminescence 160 minutes after the contact. When taken in concentrations like 0.25 mole/l (14 g/l) and 0.1 mole/l (5.6 g/l) nanoFe revealed a weak toxic effect resulting in a 30 % bioluminescence quenching 80 minutes after the contact. NanoFe concentration lying within the range of 0.05-0.000781 mole/l (2.8-0.044 g/l) showed lack of substantial impact on the microorganism bioluminescence. The data was used for detecting non-toxic nanoFe dosages in intramuscular injections.

In vivo study results

A study of the mineral composition in the animals' tissues conducted within 49 days showed certain changes in the chemical element exchange in rats, which was due to nanoFe impact. A single injection of nanoFe within the first seven days revealed that the liver had a reduced level of Mg (by 28.38%; p<0.05), K (by 22.45%; p<0.05). The concentration of the toxic elements (tin monoxide, lead, and strontium) went up. The first nanoFe injection was associated with a reduced iron concentration in the liver (by 18.25 %) (Figure 1 A, B). The Pearls qualitative histochemical reaction in the liver produced positive result only on Day 14 after 1 injection.

The experiment revealed no disturbance in the liver microstructure. However, an investigation into the dynamics of transaminase activity (AST, ALT) showed an increase in their activity. ALT activity on Day 3 after the first injection went above the controls by 69.5 % (p<0.05) (Figure 2). On Day 7 the ALT activity in the experimental group went down exceeding the control values by 29.8%. On Day 14 and Day 21 after the first injection the blood transaminase

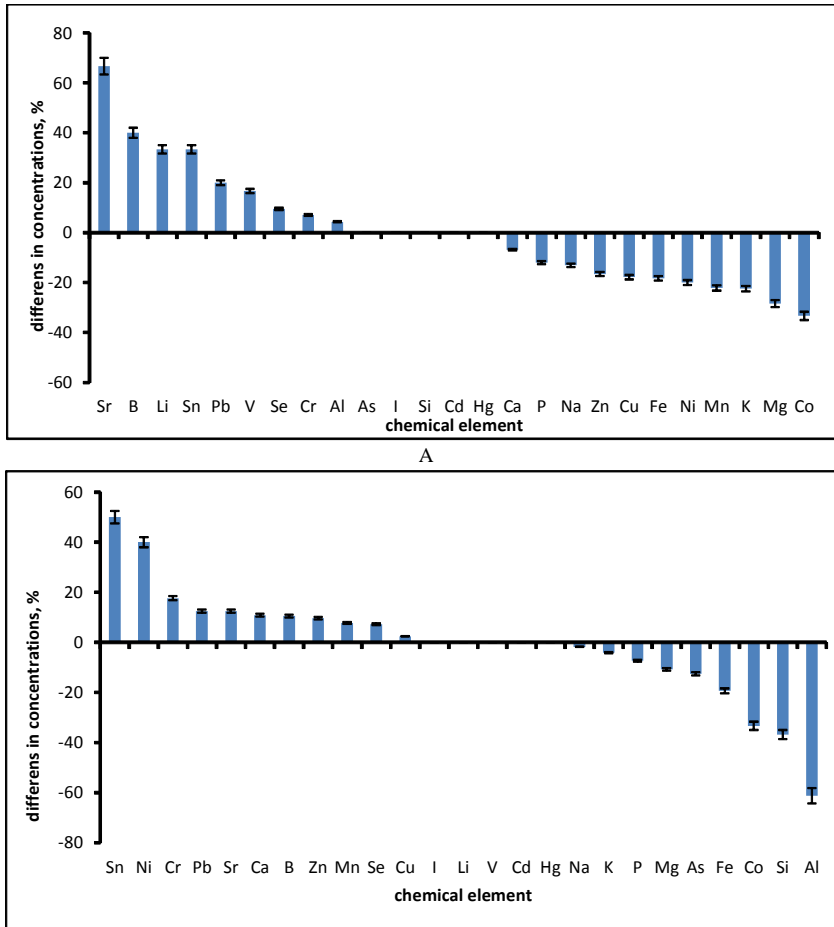


Fig. 1. Difference in the mineral element concentration in the liver of the animals, control group, 1 day after (A), and 7 days after (B) the first nanoFe injection; dosage – 2 mcg / kg, %

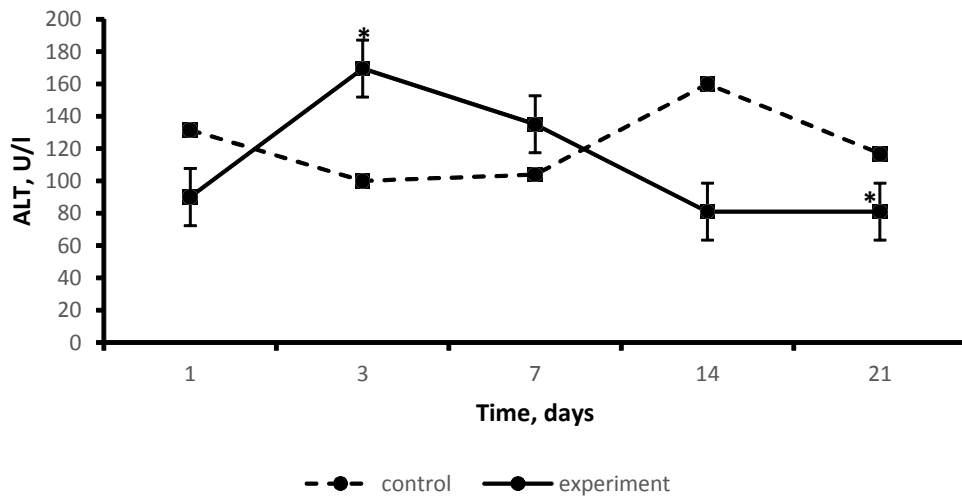


Fig. 2. ALT Levels in blood serum in rats after the 1st injection of nanoFe, dosage – 2 mg/kg, U/l

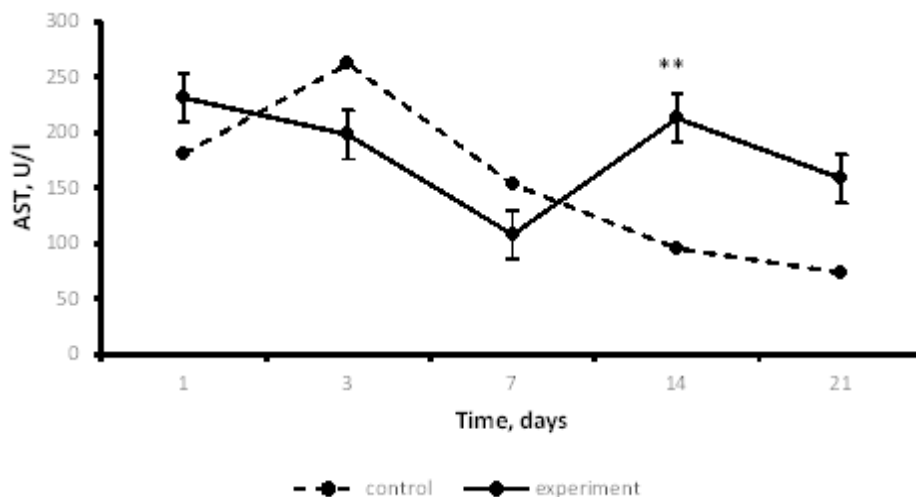


Fig. 3. Levels of AST in blood serum in rats at injecting nanoFe, dosage 2 mg/kg, U/l data presented as: mean (X) ± standard error of the mean (SE), * - results are statistically significant (p<0.05), ** - results are statistically significant (p<0.01)

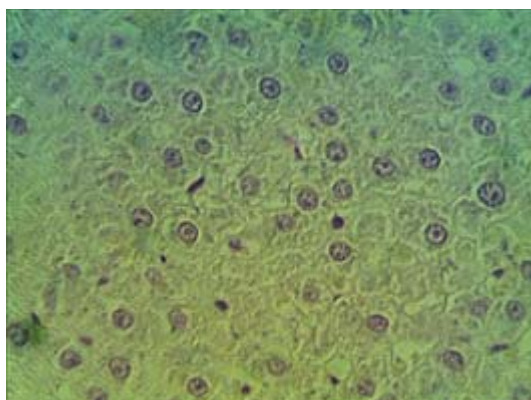


Fig. 4. Liver. Negative Pearls reaction on Day 7 after the 7th injection. Magnification – 600

activity in the experimental group was below that in the control group by 49.3% and by 30.7% ($\text{Đ} < 0.05$).

The blood transaminase activity in the rats assessed by AST went up on Day 1 of the experiment by 27.9% (Fig. 3). Later on it went down compared to the control values – by 24.4% on Day 3 and by 29.6% - on Day 7. Through the second and the third weeks of the experiment, the AST activity was above the controls – Day 14 – by 123% ($\text{Đ} < 0.01$), Day 21 – by 115%. The AST activity growth describes the nanoparticle effect as cytotoxic.

The adaptive changes in the chemical

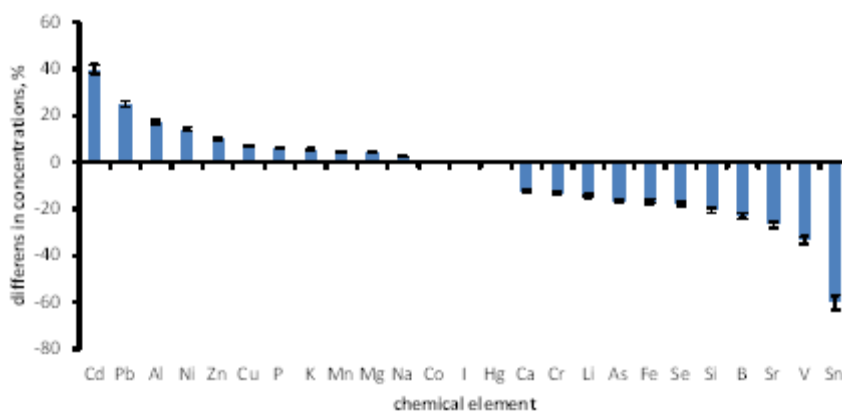


Fig. 5. Difference in the mineral element concentration in the liver of the animals, the experimental group compared to the control group, Day 7 after the 7th nanoFe injection; dosage – 2 mcg / kg, %

element exchange in the experimental group were to be observed through the entire trial. The most prominent changes were seen in iron exchange. The level of iron in the liver went down on Day 7 after the 1st injection by 19.35 % ($p < 0.05$), after the 2nd injection – by 28.9 % ($p < 0.05$), after the 3rd – by 7.01 %, after the 7th – 16.79 % ($p < 0.05$) compared to the controls.

Based on the presence of a focal proliferation after the 5th injection, we can talk about activated performance in the Kupffer cells inside some liver acini. However, by the end of the study the Kupffer reaction was negative (Figure 4).

The study showed an increase in the iron content in the blood serum in the animals involved - by 20.3% ($p < 0.001$) after 1 day; by 23.5% ($p < 0.001$) – 7 days, and by 18.8% ($p < 0.001$) 21 days after the injection

Significant changes were observed in the exchange of essential microelements Cr, Cu, B, Zn already on Day 1 after the first injection (Figure. 1). In particular, the levels of Zn on Day 1 after the injection went down by 16.57%. The next three days revealed a steady increase in the Zn content. The dynamics in the Zn concentration may be linked to an increased level of lactatedehydrogenase (LDH), which is a zinc-containing enzyme. On Day 1 of the experiment the LDH activity went up by 116.3 % ($p < 0.001$) compared to the controls. Further on, on Day 7 and Day 21 the values in the experiment and the controls got equal remaining high at 693 IU/l on Day 7, and went down back to the initial values of 377.3 IU/l in the controls and 351.5 – in the experimental group on Day 21. When analyzing the content of the macroelements Ca , Mg , Na , P in the liver It was detected that their pool (the sum of the substance amount, mole) was most stable if compared to the general microelement pool and the range of variations was 4.1 – 10.4 %. In particular, there was a decrease in the calcium concentrations in the experiment compared to the control group; a day later after the first injection the decrease was 6.81 %; on Day 7 after the 2nd injection the decrease was 18.58 % ($p < 0.05$); after the 3rd and the 4th injections – 6.1 % and 12.4 % ($p < 0.01$), respectively.

Multiple injection of nanoFe came along with changes in the content of toxic elements in

the liver. On Day 1 after the 1st injection it manifested itself through an increase in the concentration of nearly all the elements under study: Pb by 20.0 % ($p < 0.05$), Sn by 33.3% ($p < 0.05$), Sr by 66.67% ($p < 0.01$). The adaptive changes in the toxic element exchange revealed themselves in a relative decrease in their levels in the animals' liver within the first three weeks after the injection.

The most significant decrease was observed in Al – 60.5% and Sr – 76.7% compared to the control values. Seven consecutive injections of nanoFe resulted in different changes in the toxic elements content. On Day 7 after the 7th injection the level of Al went up beyond that in the control group by 17.39% ($p < 0.05$), Cd – by 40.0% ($p < 0.001$), Pb – by 25.0% ($p < 0.001$). At the same time the concentration of tin and strontium, on the contrary, went down against the control values by 60.0 % ($p < 0.0001$) and 26.67% ($p < 0.0001$), respectively.

The content of arsenic went up significantly after the 2nd injection, while the concentration difference with the third injection was by 210.3 % ($p < 0.05$). The Ni concentration at single injection of nanoparticles went down by 33.3 % ($p < 0.01$) compared to the control group; in case of multiple injections, however, there was an opposite effect – an increase by 14.29 %. The Cu concentration in the experimental group went down after the 1st injection by 17.8 %, after the 2nd injection – by 8.5 %, after the 3rd injection – by 4.2 %, and a 7 % ($p < 0.05$) increase was observed following the 7th injection.

DISCUSSION

The common practice of using iron nanoparticles¹ as well as their potential use as microelement preparations¹⁴ explain the need for investigating the impact caused by the nanoparticles on other chemical elements exchange. This need is due to the synergy and the antagonism of these elements. The study presented here serves evidence to this fact. Intramuscular injections of nanoFe were associated with changes in the chemical element exchange in the animals. Looking into the reasons behind these changes

While looking at the reasons behind these changes it must be noted that our study does not offer a description as to a prominent toxic

effect of nanoFe. This is confirmed through our study involving the model *E. coli* K12 TG1, at assessing the morphology of the liver, and in earlier works on multiple injections of nanoparticles²³.

The choice of liver as the model is due to the fact that it is one of the major depots for microelements, which are able of being involved into exchange with plasma for several hours²⁴.

In our studies multiple injections of nanoFe came along with reduced content of this element in the liver, which was rather natural. Iron concentrations in biological fluids are known to be subject to tough regulation²⁵. Excess of iron may result in generation of active forms of oxygen^{26, 27}.

Iron injected intramuscularly is deposited at the injection site to be further released gradually from the depot causing increases in hemoglobin, serum iron, and ferritin²⁸.

The development of homeostatic reaction to nanoFe injection was associated with a gradual decrease of selenium content in the liver. In particular, a week after the first injection the content of selenium in the animals' liver went beyond the control levels by 7.25%. Later on it went down steadily, compare to the controls, on Day 7 after the 2nd injection (by 1.16%), after the 3rd injection (by 6.1% ($p < 0.05$)), after the 7th injection (by 17.57% ($p < 0.01$)). Selenium consumption was detected through its involvement into compounds of selenium-proteins needed for protecting cells from oxidative materials^{29, 30, 31} as well as from heavy metals against reducing iron concentrations, which is compatible with the earlier obtained data on antagonism of these elements³². The reasons behind this include competition for common transport proteins for iron and other bivalent metals in the intestines^{33, 34}.

Earlier it has been shown that additional introduction of iron into blood is associated with ferroportin synthesis³⁵. Obviously, the capacity of ferroportin to transport other metals, too, including Cd^{36, 37} might lead to certain change in their total pool in the body.

Oxidative stress induced by nanoFe damages cells³⁸. This is why there were earlier reports about pathological processes taking place in the liver in case of introduction of nanoparticles of Fe, Ni, Zn³⁹.

Our research shows that the liver reveals no pathomorphological processes evaluated

through light visualization. However, when evaluating transaminase dynamics (AST, ALT) there was an increase in their activity detected, which might be a consequence to damaged cell membrane.

Similar results were obtained when injection rats with iron oxide nanoparticles (dosage 10 mg/kg). The nanoparticles injection were associated with increased levels of aspartate transaminase (AST), alanine transaminase (ALT), alkaline phosphatase (ALP), and gamma-glutamyltransferase (γ GT). However, histological analysis of the liver, kidneys, spleen, lungs, brain, and heart revealed no typical damage⁴⁰.

CONCLUSION

Intramuscular injections with iron nanoparticles are associated with significant changes in the animals' element status already on the first day after the injection and remain there for up to three weeks. Along with vital elements, the effect of iron nanoparticles expands to cover toxic elements as well. Studies suggest that it is advisable to perform additional correction of the element composition in diets in case of iron nanoparticles injections.

ACKNOWLEDGEMENTS

This research was done with the financial support of the Russian Science Foundation 14-16-00060

REFERENCES

1. Boyer, C., M. R. Whittaker, V. Bulmus, J. Liu and T. P. Davis, 2010. The design and utility of polymer-stabilized iron-oxide nanoparticles for nanomedicine applications. *NPG Asia Materials*, 2(1): 23-30. doi: 10.1038/asiamat.2010.6.
2. Gleich, B. and J. Weizenecker, 2015. Tomographic imaging using the nonlinear response of magnetic particles. *Nature*, 435(7046): 1214-1217.
3. Panagiotopoulos, N., R. L. Duschka, M. Ahlborg, G. Bringout, C. Debbeler, M. Graeser, C. Kaethner, K. Ldtke-Buzug, H. Medimagh, J. Stelzner, T. M. Buzug, J. Barkhausen, F. M. Vogt and J. Haegele, 2015. Magnetic particle imaging: current developments and future directions. *Int J Nanomedicine*, 22, 10: 3097-114. doi: 10.2147/IJN.S70488.

4. Estelrich, J., M. J. Sanchez-Martn and M. A. Busquets, 2015. Nanoparticles in magnetic resonance imaging: from simple to dual contrast agents. *Int J Nanomedicine*, 6, 10: 1727-1741. doi: 10.2147/IJN.S76501.
5. Zhu, Y., Y. Sun, Y. Chen, W. Liu, J. Jiang, W. Guan, Z. Zhang and Y. Duan, 2015. In Vivo Molecular MRI Imaging of Prostate Cancer by Targeting PSMA with Polypeptide-Labeled Superparamagnetic Iron Oxide Nanoparticles. *Int J Mol Sci*, 28, 16(5): 9573-87. doi: 10.3390/ijms16059573.
6. Jordan, A., R. Scholz, K. Maier-Hauff *et al.*, 2001. Presentation of a new magnetic field therapy system for the treatment of human solid tumors with magnetic fluid hyperthermia. *Journal of Magnetism and Magnetic Materials*, 225(1-2): 118-126. doi: 10.1016/S0304-8853(00)01239-7.
7. Dobson, J., 2010. Cancer therapy: a twist on tumour targeting. *Nature Materials*, 9(2): 95-96. doi: 10.1038/nmat2604.
8. Sadeghi, L., F. Tanwir and V. Yousefi Babadi, 2014. In vitro toxicity of iron oxide nanoparticle: Oxidative damages on Hep G2 cells. *Exp Toxicol Pathol*, pii: S0940-2993(14)00180-8. doi: 10.1016/j.etp.2014.11.010.
9. Vellayappan, M. V., A. Balaji, A. P. Subramanian, A. A. John, S. K. Jaganathan, S. Murugesan, E. Supriyanto and M. Yusof, 2015. Multifaceted prospects of nanocomposites for cardiovascular grafts and stents. *Int J Nanomedicine*, 7, 10: 2785-2803. doi: 10.2147/IJN.S80121.
10. Estelrich, J., E. Escribano, J. Queralt and M. A. Busquets, 2015. Iron oxide nanoparticles for magnetically-guided and magnetically-responsive drug delivery. *Int J Mol Sci*, 10, 16(4): 8070-1801. doi: 10.3390/ijms16048070.
11. Aslam, M. F., D. M. Frazer, N. Faria, S. F. Bruggaber, S. J. Wilkins, C. Mirciov, J. J. Powell, G. J. Anderson, D. I. Pereira *et al.*, 2014. Ferroportin mediates the intestinal absorption of iron from a nanoparticulate ferritin core mimetic in mice. *FASEB J*, 28(8): 3671-3678. doi: 10.1096/fj.14-251520.
12. Prietl, B., C. Meindl, E. Roblegg, T. R. Pieber, G. Lanzer and E. Frhlich, 2014. Nano-sized and micro-sized polystyrene particles affect phagocyte function. *Cell Biol Toxicol*, 30(1): 1-16. doi: 10.1007/s10565-013-9265-y.
13. Lozano-Fernndez, T., L. Ballester-Antxordoki, N. Prez-Temprano, E. Rojas, D. Sanz, M. Iglesias-Gaspar, S. Moya, A. Gonzlez-Fernndez and M. Rey, 2014. Potential impact of metal oxide nanoparticles on the immune system: The role of integrins, L-selectin and the chemokine receptor CXCR4. *Nanomedicine*, 10(6): 1301-1310. doi: 10.1016/j.nano.2014.03.007.
14. Vermeij, E. A., M. I. Koenders, M. B. Bennink, L. A. Crowe, L. Maurizi, J. P. Valle, H. Hofmann, W. B. Van Den Berg, P. L. Van Lent and F.A. Van De Loo, 2015. The in-vivo use of superparamagnetic iron oxide nanoparticles to detect inflammation elicits a cytokine response but does not aggravate experimental arthritis. *PLoS One*, 8, 10(5): e0126687. doi: 10.1371/journal.pone.0126687.
15. Chen, P. J., C. H. Su, C. Y. Tseng, S. W. Tan and C. H. Cheng, 2011. Toxicity assessments of nanoscale zerovalent iron and its oxidation products in medaka (*Oryziaslatipes*) fish. *Mar Pollut Bull*, 63(5-12): 339-346. doi: 10.1016/j.marpolbul.2011.02.045.
16. Wang, H., J. Zhang and H. Yu, 2007. Elemental selenium at nano size possesses lower toxicity without compromising the fundamental effect on selenoenzymes: comparison with selenomethionine in mice. *Free Radic Biol Med*, 42: 1524-1533. doi: 10.1016/j.freeradbiomed.2007.02.013.
17. Xu, B. H., Z. L. Xu and M. S. Xia, 2003. Effect of nano red elemental selenium on GPx activity of broiler chick kidney cells in vitro. *Wuhan Univ J Nat Sci*, 8: 1167-1172. doi: 10.1007/BF02903693.
18. Zhang, J. S., H. L. Wang, X. X. Yan and L. D. Zhang, 2005. Comparison of short-term toxicity between nano-Se and selenite in mice. *Life Sci*, 76: 1099-1109. doi: 10.1016/j.lfs.2004.08.015.
19. Zhang, J. S., X. F. Wang and T. W. Xu, 2008. Elemental selenium at nano size (Nano-Se) as a potential chemopreventive agent with reduced risk of selenium toxicity: comparison with Se-methylselenocysteine in mice. *ToxicolSci*, 101: 22-31. doi: 10.1093/toxsci/kfm221.
20. Zhigach, A. N., I. O. Leipunsky, M. L. Kuskov, N. I. Stoenko and V. B. Storozhev, 2000. Plant for production and study of physical and chemical properties of metal nanoparticles / Moscow, Instruments and Experimental Techniques, 6: 122-127.
21. Klishov, A. A., 1984. Histogenesis and tissue regeneration. - D.: Meditsina. 232 p.
22. Pierce, E., 1962. Histochemistry. Theoretical and applied. Moscow. - M.: Science in Russia. 215 p.
23. Yun, J. W., S. H. Kim, J. R. You, W. H. Kim, J. J. Jang, S. K. Min, H. C. Kim, D. H. Chung, J. Jeong, B. C. Kang and J. H. Che, 2015. Comparative toxicity of silicon dioxide, silver and iron oxide nanoparticles after repeated oral

- administration to rats. *J Appl Toxicol*, 35(6): 681-93. doi: 10.1002/jat.3125.
24. Leggett, R. W., 2012. A biokinetic model for zinc for use in radiation protection. *Sci Total Environ*, 420: 1–12.
 25. Lichtman, M. A., 2006. *Williams Hematology*. McGraw-Hill Professional, p. 516.
 26. Braun, V. and H. Killmann, 1999. Bacterial solution to the iron-supply problem. *Trends Biochem Sci*, 24: 104–109.
 27. Lieu, P. T., M. Heiskala, P. A. Peterson, and Y. Yang, 2001. The roles of iron in health and disease. *Mol Aspects Med*, 2: 1–87.
 28. Sizova, E., S. Miroshnikov, E. Yausheva and V. Polyakova, 2015. Assessment of morphological and functional changes in organs of rats after intramuscular introduction of iron nanoparticles and their agglomerates. *Biomed Res Int*, 243173. doi: 10.1155/2015/243173.
 29. Hoekstra, W. G., 1975. Biochemical function of selenium and its relation to vitamin E. *Fed Pro*, 34: 2083–2090.
 30. Segalés, J., G. M. Allan and M. Domingo, 2005. Porcine circovirus diseases. *Ani Health Res Rev*, 6: 119–142. doi: 10.1079/AHR2005106.
 31. Yu, H. J., J. Q. Liu, A. Böck, J. Li, G. M. Luo and J. C. Shen, 2005. Engineering glutathione transferase to a novel glutathione peroxidase mimic with high catalytic efficiency. *JBiolChem*, 280: 11930–11935. doi: 10.1074/jbc.M408574200.
 32. Wang, Y., Y. L. Ou, Y. Q. Liu, Q. Xie, Q. F. Liu, Q. Wu, T. Q. Fan, L. L. Yan and J. Y. Wang, 2012. Correlations of trace element levels in the diet, blood, urine, and feces in the Chinese male. *Biol Trace Elem Res*, 145(2): 127-35. doi: 10.1007/s12011-011-9177-8.
 33. Ranganathan, P. N., Y. Lu, L. Jiang, C. Kim and J. F. Collins, 2011. Serum ceruloplasmin protein expression and activity increases in Iron-deficient rats and is further enhanced by higher dietary copper intake. *Blood*, 118(11): 3146–3153.
 34. Barany, E., I. A. Bergdahl, L-E. Bratteby et al., 2005. Iron status influences trace element levels in human blood and serum. *Environmental Research*, 98(2): 215–223.
 35. Delaby, C., N. Pilard, A. S. Goncalves, C. Beaumont and F. Canonne-Hergaux, 2005. Presence of the iron exporter ferroportin at the plasma membrane of macrophages is enhanced by iron loading and down-regulated by hepcidin. *Blood*, 106: 3979–3984.
 36. Troadec, M. B., D. M. Ward, E. Lo, J. Kaplan and I. De Domenico, 2010. Induction of FPN1 transcription by MTF-1 reveals a role for ferroportin in transition metal efflux. *Blood*, 116: 4657–4664.
 37. Chung, J., D. J. Haile and M. Wessling-Resnick, 2004. Copper-induced ferroportin-1 expression in 774 macrophages is associated with increased iron efflux. *Proc Natl Acad Sci USA*, 101: 2700–2705.
 38. Keenan, C. R., R. Goth-Goldstein, D. Lucas and D. L. Sedlak, 2009. Oxidative stress induced by zero-valent iron nanoparticles and Fe(II) in human bronchial epithelial cells. *Environ Sci Technol*, 43(12): 4555-4560.
 39. Dudakova, Yu. S., 2009. Study the toxic effect of superfine powders of metals. *Allergology and Immunology*, 10(2): 308.
 40. Rajan, B., S. Sathish, S. Balakumar and T. Devaki, 2015. Synthesis and dose interval dependent hepatotoxicity evaluation of intravenously administered polyethylene glycol-8000 coated ultra-small superparamagnetic iron oxide nanoparticle on Wistar rats. *Environ Toxicol Pharmacol*, 39(2): 727-735. doi: 10.1016/j.etap.2015.01.018.